Available online at www.sciencedirect.com
ScienceDirect
Journal of Magnetic Resonance 183 (2006) 68–76
JMR Journal of Magnetic Resonance
www.elsevier.com/locate/jmr

Polarization transfer from remote protons in ^{13}C CP/MAS

Carmen Tripon [a], Mihaela Aluas [b], Xenia Filip [a], Claudiu Filip [a,*]

[a] National Institute for R&D of Isotopic and Molecular Technologies, P.O. Box 700, 400293 Cluj, Romania
[b] Physics Department, Babes-Bolyai University, Cluj, Romania

Received 23 June 2006; revised 14 July 2006
Available online 17 August 2006

Abstract

An experimental procedure for CP/MAS polarization transfer from remote ^1H nuclear spins is introduced, which is applicable to protonated carbons in organic solids. It is based on preparing a state of non-uniform polarization, where directly bonded ^{13}C–^1H nuclei are de-polarized prior to recording the CP buildup curve. This curve is then expected to quantify the polarization transfer from remote protons only. The ability of the cross-polarization/polarization-inversion (CPPI) sequence to generate an initial state suitable for remote ^1H CP/MAS scheme is analyzed both theoretically and experimentally. Confining to aliphatic groups, it was found that complete de-polarization of bonded proton is possible in the case of CH, whereas for CH_2 and CH_3 moieties only a partial de-polarization can be achieved. The theoretical predictions have been verified in practice for the particular case of L-alanine. The significance of the results from fundamental, as well as practical point of view, is also discussed. In particular, it is shown that: (i) the coherent description of polarization transfer under CP/MAS, including ^1H polarization redistribution, is valid over time-scales longer than commonly assumed in many treatments of cross-polarization, and (ii) the remote protons polarization transfer curve can be used in combination with the conventional CP/MAS curve to get additional structural and dynamical information in organic systems.

Keywords: Solid-state NMR; Cross-polarization; CP/MAS; Spin dynamics

1. Introduction

The combination of cross-polarization (CP) [1] with high-power proton decoupling and magic angle spinning (MAS) [2] is routinely used for increasing sensitivity in high-resolution solid-state nuclear magnetic resonance (SS-NMR) spectroscopy of low-γ nuclear spins (^{13}C, ^{15}N) in organic materials. CP is performed under simultaneous irradiation with strong resonant rf fields of ^1H and low-γ nuclei (designated here by the I and S spin, respectively). An optimum polarization transfer between the two spin species is attained at exact Hartmann–Hahn matching [1,3].

The transfer process has been described using thermodynamic [4,5] as well as quantum-mechanical treatments [6–10]. In thermodynamic models, CP is viewed as a process of thermal equilibration between the I spin and S spin reservoirs (via the I–S heteronuclear dipolar interaction), which is parameterized through a CP transfer rate, T_{IS}^{-1} [4]. A modified spin thermodynamic theory has also been developed [5] to describe the amount of transferred polarization under different experimental conditions in terms of quasi-invariant operators associated to the CP process. The deterministic nature of cross-polarization, clearly demonstrated by time-reversal CP [11], has been accounted for in many quantum-mechanical treatments. This was done by Demco et al. [6] for the static case based on a memory function approach, and resulted in an explicit dependence of the T_{IS}^{-1} rate on I–S dipolar coupling parameters. Generalization to the CP/MAS case was done by Stejskal et al. [7], whereas a detailed quantum treatment in terms of energy level matching in the Hilbert (and Hilbert–Floquet space for CP/MAS) was performed by Marks and Vega [8]. The offset and CSA effects upon CP dynamics have also been thoroughly investigated [9,10].

* Corresponding author. Fax: +40 264 420042.
E-mail address: cfilip@s3.itim-cj.ro (C. Filip).

1090-7807/$ - see front matter © 2006 Elsevier Inc. All rights reserved.
doi:10.1016/j.jmr.2006.07.019

The thermodynamic picture is usually applied to systems with strong I–I couplings, where the evolution of the transferred polarization with the CP contact time can be described through a single exponential function. By contrast, when the dipolar coupling between directly bonded I–S spins exceeds the I–I couplings, as in the case of protonated ^{13}C, the CP curve evolves in a damped oscillatory fashion, giving rise to the so-called transient oscillations [12]. This phenomenon is considered a clear indication of the coherent nature of the polarization transfer process, and it has been extensively used for extracting structural and dynamical information in organic solids, liquid crystals, and oriented membrane proteins. Important applications emerged in recent years once more sophisticated coherent manipulation schemes of the polarization transfer process, such as polarization inversion spin exchange at the magic angle (PISEMA) [13], have been introduced: this generally leads to better shaped transient oscillations and, consequently, increased accuracy in extracting structural information—see Ref. [14] for a review on this topic. Most of the applications rely on measuring heteronuclear dipolar couplings with ^{13}C chemical site resolution by means of 2D separated local field (SLF) spectroscopy [15]. For dipolar mixing, a large variety of sequences were demonstrated, from the conventional CP/MAS, to cross-polarization/polarization inversion (CPPI) [16], Lee-Goldburg cross-polarization, (LG-CP) [17–21], Phase Inverted LG Recoupling under MAS (PILGRIM) [22], PISEMA [13], with its modified versions PISEMA-MAS [17], PITANSEMA [23], PITANSEMA-MAS [24], and Heteronuclear Isotropic Mixing leading to spin Exchange via the Local Field (HIMSELF) [25,26].

For every ^{13}C chemically distinct site, the dipolar spectra measured through 2D SLF spectroscopy are dominated by the strongest C–H couplings, with smaller effects coming also from more distant protons. In principle, each individual contribution can be separated according to its ^{1}H chemical shift value by means of 3D LG-CP HETCOR [19,27–30]. However, this is not a generally valid procedure due to the strong dependence on the achievable proton resolution.

In the present work we introduce a simplified scheme for separating distinct contributions to the CP/MAS curve (thus, implicitly, to the C–H dipolar spectrum), which relies on the large difference in polarization dynamics between directly bonded, and remote ^{1}H spins, respectively. As such, it is applicable to the particular case of protonated carbons in organic solids, where we demonstrate the possibility of recording CP/MAS buildup curves that quantify mainly the polarization transfer from remote protons. This scheme is implemented in practice using a CPPI sequence. A theoretical analysis of the underlying CP dynamics is performed, which is then verified by the experimental results acquired on L-alanine.

2. General principles

The dynamics of cross-polarization [6] is usually analyzed in a doubly tilted frame, of which z axes are aligned along the direction of the spin-locking fields, ω_{1I} and ω_{1S}, and also, in an interaction picture with respect to the dominant term, $\omega_{1I}I_z + \omega_{1S}S_z$. In the following, one considers the polarization transfer process at the first Hartmann–Hahn matching condition ($\omega_{1I} - \omega_{1S} = \omega_R$) in a system composed of a single S spin (^{13}C) surrounded by abundant I (^{1}H) spins. As demonstrated in Ref. [19], the lowest order approximation, i.e., the truncation of the total Hamiltonian to its static terms, is sufficient to describe the main features of CP/MAS dynamics under fast sample spinning. These static terms are given by

$$\tilde{H}_{\mathrm{int}}(t) = \sum_{j=1}^{N} b_j \left(I_{j+} S_- \mathrm{e}^{\mathrm{i}\varphi_j} + I_{j-} S_+ \mathrm{e}^{-\mathrm{i}\varphi_j} \right) \tag{1}$$

where

$$b_j = -\frac{\mu_0}{4\pi} \frac{h\gamma_I\gamma_S}{r_j^3} \frac{\sqrt{2}}{4} \sin 2\theta_j \tag{2}$$

is the recoupled part of the dipolar interaction, with r_j, the I_j–S distance, and (θ_j, ϕ_j), the azimuthal and polar angles of the corresponding inter-nuclear vector in the rotor frame. The contribution of the I_j spin to the transferred S-spin polarization is given by

$$S_j(t) = \langle S_z | \mathrm{e}^{-\mathrm{i}\hat{\tilde{H}}_{\mathrm{int}} t} | I_{jz} \rangle \tag{3}$$

Its exact analytical evaluation has been performed [19] in the case of an SI_2 spin system. It was found that

$$S_j(t) \sim \left\langle \frac{b_j^2}{\omega^2} \sin^2 \omega t \right\rangle \tag{4}$$

where $\langle \cdots \rangle$ represents the average over the all possible orientations, and

$$\omega = \sqrt{b_1^2 + b_2^2} \tag{5}$$

The summation over the individual j contributions, obviously gives the total polarization transferred to the S spin in a classical CP/MAS experiment, i.e.,

$$S(t) \sim \sum_{j=1,2} \left\langle \frac{b_j^2}{\omega^2} \sin^2 \omega t \right\rangle = \langle \sin^2 \omega t \rangle \tag{6}$$

The above relationships suggest that the polarization acquired by the S spin under the action of the Hamiltonian (1) brakes into independent I_j–S components, of which contributions to the total signal strongly depend on the corresponding dipolar couplings, through the $(b_j/\omega)^2$ scaling factor. Such dependence cannot be distinguished in a conventional CP/MAS curve, because this is acquired based on an initial state of uniform ^{1}H polarization, thus giving rise to a ^{13}C signal of the form (6). The I_j–S components can be separated instead if starting from an initial state of non-uniform proton polarization. For instance, this is done in 3D LG-CP HETCOR [19,27–30], where the decomposition is in principle complete. In practice, however, well resolved absorption lines along the ^{1}H

dimension are required for achieving this goal. Here, it is demonstrated that partial separation of different contributions to the total CP/MAS signal can be obtained also by using an experimental setup which does not depend on the achievable proton resolution. In particular, we confine to the case of protonated carbons in organic solids, and investigate the possibility of removing the dominant contribution of directly bonded ^{1}H nuclei from measured ^{13}C CP/MAS curves. These new buildup curves are thus expected to quantify the polarization transfer process from the remote protons only.

The experimental approach is based on generating an initial state of non-uniform ^{1}H polarization by employing a CPPI scheme similar to that used in the past for SLF spectroscopy [16], and spectral editing [31]. As can be seen in Fig. 1, the setup consists of three distinct CP blocks, where the phase of the second proton contact pulse is reversed with respect to the first and the third pulse. The first two CP blocks of fixed durations, τ_1 and τ_2 (i.e., the CPPI sequence) act as a preparation period, during which the desired state of non-uniform ^{1}H polarization is generated. This sequence is followed by a dephasing period, τ_{deph}, which is included with the purpose of removing the effect of unwanted spin correlations. The CP buildup curve corresponding to the initial state prepared in this way is recorded by incrementing the third CP contact pulse, τ_{CP}.

To get buildup curves that quantify mainly the polarization transfer from non-bonded (remote) protons there are two important conditions to be met: (i) the CPPI sequence should *simultaneously* bring to zero the polarization of the central carbon and of its bonded protons, while also keeping significant polarization on the remote protons, and (ii) the influence of other spin-correlations (besides the remote protons polarization) present in the initial state prepared by the CPPI sequence should be made negligible small. The extent to which these requirements are fulfilled in the particular case of aliphatic groups is quantitatively analyzed below by numerical simulations. The computations are performed on representative C-H7 spin systems using the *Spinevolution* program [32]. In particular, for CH and CH_3 groups we use the specified ^{13}C spin surrounded by the seven protons in L-alanine, whereas for CH_2 one considers the five intra-molecular protons in glycine, and also the closest two inter-molecular ^{1}H spins (which belong to a CH_2 group). The corresponding atomic coordinates have been extracted from their reported crystal structures [33,34].

The evolution of spin polarization with increasing the inversion time in the CPPI sequence, τ_2, is shown in Fig. 2 at three distinct spinning frequencies, $\nu_R = 5$, 8, and 15 kHz. For each of the investigated systems, the first CP block has a fixed duration corresponding to maximum polarization transferred from the bonded ^{1}H nuclei, namely $\tau_1 = 70$, 60, and 185 μs, for the CH, CH_2, and CH_3 group, respectively. The ^{13}C polarization is drawn by thick line, the bonded protons polarization by thin line, whereas the dashed lines correspond to the remote ^{1}H polarization. A close inspection of these dependencies clearly demonstrates that one can simultaneously bring to zero the carbon and the bonded proton polarization only in the case of the CH group (at 8 kHz spinning frequency, and an inversion time τ_2 of 42 μs). For the other two aliphatic groups, the condition (i) is only partially fulfilled, because the cancellation of the ^{13}C polarization is accompanied by a finite polarization left on the bonded ^{1}H spins, which is proportional with their number. With respect to the polarization left on the remote protons at the moment τ_2 of ^{13}C polarization inversion, one can consider it sufficiently high to give significant transfer signal in all investigated systems.

Thus, in the case of CH moiety, the CPPI sequence is well suited for preparing the initial state required by the experimental scheme depicted in Fig. 1. The CP buildup curve obtained by increasing τ_{CP} is expected to quantify here only the transfer from remote protons. The CH_2, and CH_3 curves will be instead "contaminated" with polarization transferred from bonded protons, in an amount which depends on its remnant value at the end of the preparation time. Therefore, the analysis of the condition (ii) stated above will be confined to the CH case. This is illus-

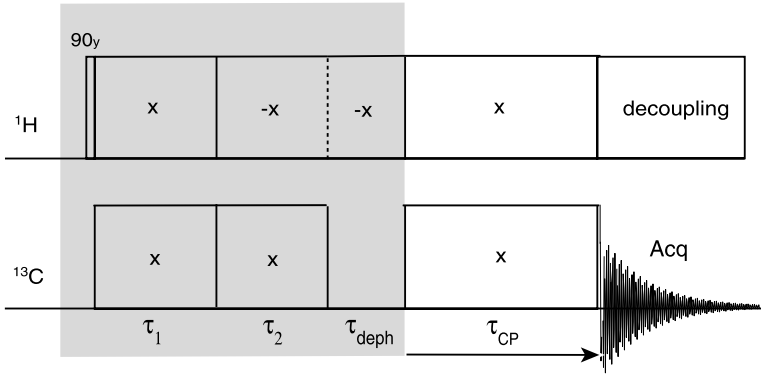

Fig. 1. The pulse sequence employed for the remote protons polarization transfer scheme. It consists of a preparation period (shaded area), followed by a standard CP/MAS sequence. The remote protons CP/MAS curve is recorded by incrementing the value of the third contact time, τ_{CP}. Alternating the phase of the first two proton contact pulses (the CPPI sequence) an initial state with zero polarization on both, the ^{13}C and its bonded ^{1}H is prepared. A dephasing period, τ_{deph}, has been also added with the purpose of removing additional (unwanted) spin correlations.

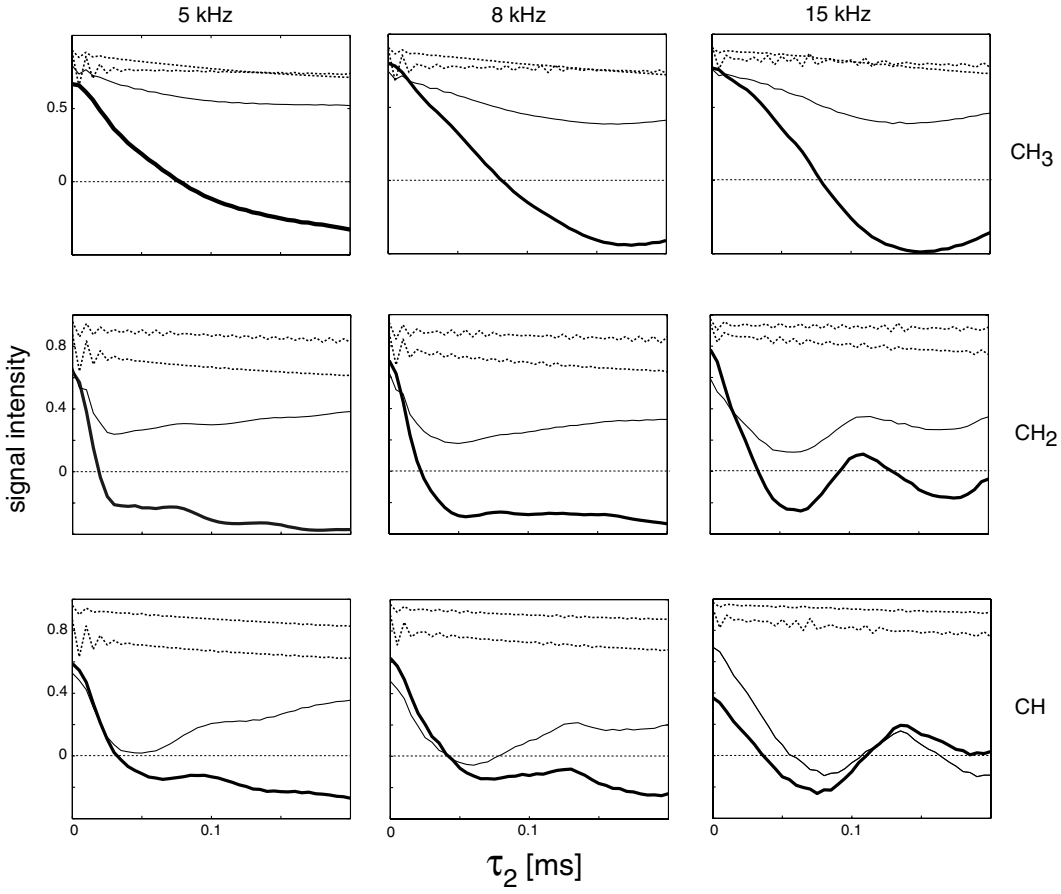

Fig. 2. Simulated spin polarization dependencies on the inversion time τ_2 in the CPPI sequence at $\nu_R = 5$, 8, and 15 kHz spinning frequencies. For each of the illustrated moiety, they are performed on representative C-H7 spin systems by using appropriate values of τ_1, as described in the text. By continuous lines are shown the polarization inversion curves of the central ^{13}C (thick line), and of its directly bonded ^{1}H (thin line). By dashed lines is drawn the polarization left on the non-bonded (remote) ^{1}H spins. Specifically, they are represented by the (CH_3, NH_3), (CH_3, inter-molecular CH_2), and (CH, NH_3) protons for CH, CH_2, and CH_3, respectively.

trated in Fig. 3 by comparing two CP curves, which are generated from the same non-uniform distribution of spin polarization, but employing different experimental schemes. The polarization on each spin in the system is chosen here to coincide with that produced by a CPPI sequence where τ_1 and τ_2 are set to 70, and 42 μs, respectively—see the figure caption for details. In the first case (thick line), this non-uniform polarization is simply used as an initial state in a conventional CP/MAS experiment. This imaginary experiment gives an ideal CP curve, which, in practice, should be approached as much as possible for achieving efficient remote protons polarization transfer. To get a real CP curve (thin line), however, the CPPI sequence has to be explicitly included into the simulations as a preparation period. The dephasing time was set to $\tau_{deph} = 50$ μs, and the spinning frequency to $\nu_R = 8$ kHz. Besides the desired differential spin polarization, this sequence is expected to generate also unwanted spin correlations.

In Fig. 3a, the computed CP curves corresponding to the two distinct experimental conditions are represented for τ_{CP} ranging from 0 to 3 ms. Although both follow the same general trend, small differences still exist between them. In particular, a slightly lower saturation level is reached by the transferred polarization in the real case compared to the ideal one, and also, small oscillations are superimposed over the real CP curve, whereas the ideal curve shows a relatively smooth evolution. The oscillations are more clearly evidenced in Fig. 3b, which expands the short-time region (0–0.5 ms) of the previous figure. Despite these effects of the spurious spin correlations generated by the CPPI sequence, the deviation of the real CP curve from the ideal behavior is not very significant: thus, in a first approximation, it describes the remote protons polarization transfer process fairly well.

Important conclusions with respect to possible applications of the proposed scheme to structural refinement in organic systems can be drawn from a comparison between the remote protons polarization transfer curve and the curve obtained by conventional CP/MAS, i.e., starting from uniform spin polarization (dashed line in Fig. 3a). According to the relationships (4) and (6), both of them evolve with the same dipolar oscillation frequency, but the former can provide additional structural information

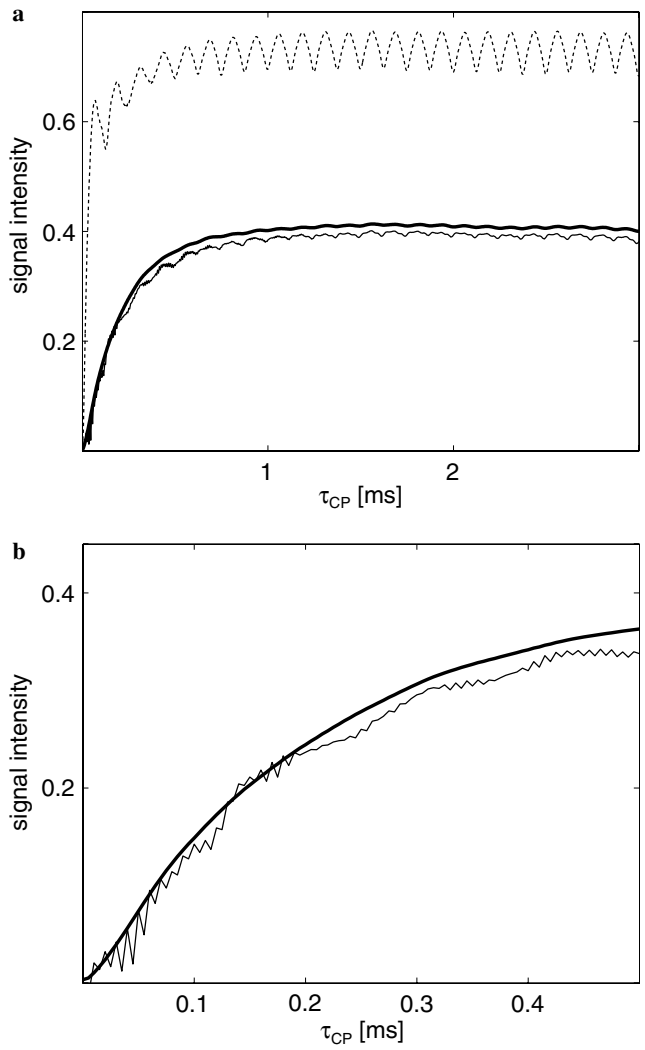

Fig. 3. Simulated remote protons CP/MAS curves of the CH group performed on the C-H7 spin system at $\nu_R = 8$ kHz. An ideal curve (thick line) is obtained by standard CP/MAS starting from an initial state of non-uniform spin polarization—this represents an imaginary experiment where the effect of the preparation period is only *implicitly* assumed. The employed polarization distribution, i.e., $S_z = 0$ (the CH carbon), $I_z = 0$ (the CH proton), $I_z = 0.95$ (the CH_3 protons), and $I_z = 0.77$ (the NH_3 protons) is the same as the distribution that would be produced by a CPPI sequence with $\tau_1 = 70$ and $\tau_2 = 42$ μs. The real curve (thin line) is obtained starting from an initial state of uniform spin polarization, but by *explicitly* incorporating the preparation sequence in the simulations. For comparison, the conventional CP/MAS curve (dashed line) is also shown in (a). In (b), it is illustrated an expansion of the short-time region (0–0.5 ms).

through the scaling factor $(b_j/\omega)^2$, which explicitly incorporates the distances to the remote protons. As shown in Ref. [19], this scaling will affect the saturation level, as well as the buildup rate of the corresponding transfer curve. These features can be clearly distinguished in Fig. 3a. For instance, the remote protons CP curve is characterized by a slower buildup rate, in agreement with the reduced dipolar couplings between the CH carbon and the more distant ^{1}H spins (in our example, the CH_3 and NH_3 protons). In the case of the saturation level, one has also to consider the dependence on the number of non-bonded protons that significantly contribute to the polarization transfer process within the investigated time scale.

For practical purposes, such multiple spin effects should be appropriately taken into account. In particular, they determine a global character to the structural and dynamical information encoded into the measured remote ^{1}H CP/MAS curve, which will therefore reflect only an averaged effect of the proton environment. Still, the proposed approach could add useful structural details to the information provided by conventional CP/MAS in many cases of practical interest, for instance when poor proton resolution prevents us from using the 3D LG-CP HETCOR technique [19,27–30]. In such cases, the experimental setup can be further improved, e.g., one can perform active proton decoupling by replacing the Hartmann–Hahn CP with Lee-Goldburg CP. However, before attempting to better characterize a range of possible applications for the remote protons CP/MAS scheme, a more important issue to investigate here is the reliability and accuracy level that can be reached through its proposed experimental implementation. This will be done in the remainder of the present work by comparing the experimental and computed results on L-alanine, i.e., on a system with very well-known structure [33].

3. Experimental

Solid state ^{13}C NMR spectra were recorded at 100 MHz ^{13}C Larmor frequency with a Bruker AVANCE-400 spectrometer. All NMR experiments were performed on L-alanine at room temperature. The sample was purchased from Alfa Aesar and used without further purification. It was center-packed to minimize the effect of rf field inhomogeneity. Standard cross-polarization magic angle spinning (CP/MAS) experiments were performed at a spinning frequency $\nu_R = 8$ kHz, using a ^{1}H 90° pulse length of 3.8 μs. The ^{13}C NMR spectra were acquired under two-pulse phase-modulated (TPPM) ^{1}H decoupling at 70 kHz by averaging 256 scans with a recycle delay of 3 s.

The CP transfer was optimized for the first Hartmann–Hahn matching condition ($\nu_{1C} = \nu_{1H} - \nu_R$), where the rf fields on the ^{1}H and ^{13}C channels have been calibrated to 50 and 42 kHz, respectively. The conventional CP curves were acquired through the standard CP/MAS sequence, whereas the experimental setup illustrated in Fig. 1 has been employed for acquiring the remote protons CP/MAS curves. In both cases, the evolution of spin polarization is obtained by incrementing the length of the appropriate contact pulse from 0 to 5 ms: this was done in steps of 5 μs at short times, while at longer times the increment value has been progressively increased, so that in the end a total number of 64 points was employed to define the measured CP buildup curves.

The conventional ^{13}C CP/MAS curves have been acquired in a single experiment, with the carrier frequency set in the middle between the CH and CH_3 resonances. Since they are separated by only 3 kHz, the induced offset

effect can be considered negligible. In the case of the remote protons CP/MAS curves, two distinct experiments were carried out, because of the different preparation conditions characteristic to the two aliphatic moieties. Corresponding to the CH and CH_3 groups, the duration of the contact pulses in the CPPI sequence were found to be $\tau_1 = 70$, and 175 μs, and $\tau_2 = 47$, and 80 μs, respectively. The former was determined as the short-time maximum of the conventional CP/MAS curve, whereas the latter represents the inversion time of the ^{13}C signals in the corresponding CP polarization inversion experiment (performed separately, for each resonance). The dephasing period was set to $\tau_{deph} = 50$ μs.

4. Results and discussion

In this section, one compares the predictions of the above theoretical analysis with the experimental results. To get reliable conclusions, however, a high accuracy level is required for describing the polarization transfer process by means of numerical simulations on suitably selected spin subsystems. From this point of view, L-alanine represents an ideal model system. In particular, the precise value of the proton positions (±0.003 Å) determined by neutron diffraction [21] removes possible errors due to uncertainties in the involved C–H and H–H dipolar couplings. Also, the fast (compared with the CP time-increment, $\Delta\tau_{CP} = 5$ μs) methyl rotation around its symmetry axis has been explicitly accounted for in computations, as described in the *Spinevolution* reference manual [32].

Unlike CH_3, the strength of the hydrogen bonding network formed by NH_3^+ will generally determine high activation energies for its rotational motion and, implicitly, slower hoping rates around the symmetry axis. In the case of L-alanine [35], the corresponding hoping time becomes comparable with $\Delta\tau_{CP}$, so that special caution is needed when describing the NH_3 contribution to the CP dynamics. As such, the measured CP/MAS curves of the CH carbon are compared in the Figs. 4 and 5 with simulations performed under both, rigid approximation, and fast rotation limit of the NH_3 group, respectively. To get a feeling about the errors one might expect when working on a reduced number of spins, the results on the C-H7 spin arrangement used in the Section 2 are supplemented here with simulations performed on an extended C-H9 system, which incorporates two extra CH intermolecular protons (located at 3.5 and 3.8 Å from the central CH ^{13}C spin). The effect of the spin-lattice relaxation in the rotating frame is accounted for by multiplying the computed buildup curves with exponential functions; their decay rates have been extracted from the exponential fit of the long-time evolution in the corresponding experimental curves. Also, to enable direct comparison between experiment and theory, a suitable scaling factor had to be applied upon the measured CP/MAS curves: its value was determined from the best fit between the short-time (0–100 μs) parts of the experimental and simulated curves acquired by conventional CP/MAS. The scaling factor determined in this way was then applied upon the measured remote protons CP/MAS curve. The reported intensities correspond to CP/MAS starting from unit proton polarization.

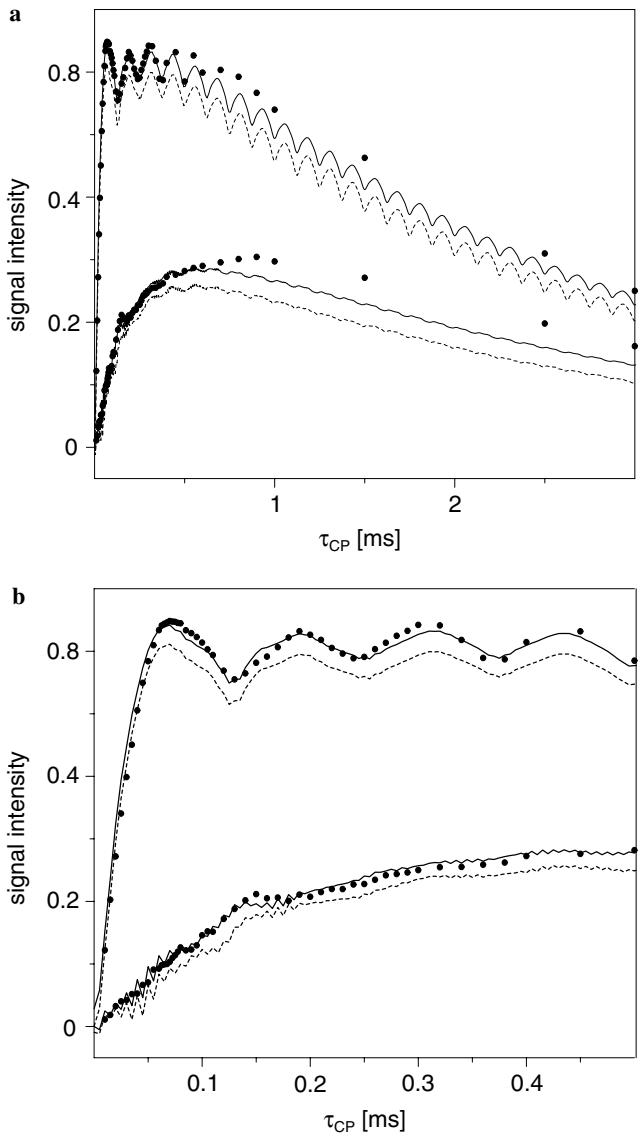

Fig. 4. Comparison between the experimental and computed buildup curves of the CH carbon in L-alanine acquired by conventional- (the upper curves), and remote protons CP/MAS (the lower curves). Measured data are represented by filled symbols: they have been collected as described in Section 3. Simulations performed in representative C-H7 (dashed line) and C-H9 (continuous line) spin subsystems (see the text for details), are both shown for comparison. Rapid rotation around the trigonal axis is considered here only for the CH_3 moiety, whereas the contribution of the NH_3 group to CP dynamics is treated in the rigid approximation. The reported signal intensities correspond to CP/MAS starting from unit proton polarization in the investigated subsystems. The illustrated dependencies for τ_{CP} in the range 0–3, and 0–0.5 ms, are shown in the figures (a), and (b), respectively.

The dependencies depicted in Figs. 4 and 5 clearly show that the correspondence between the theoretical and experimental data is much better in the rigid NH_3 approximation than in the fast rotational regime. However, small

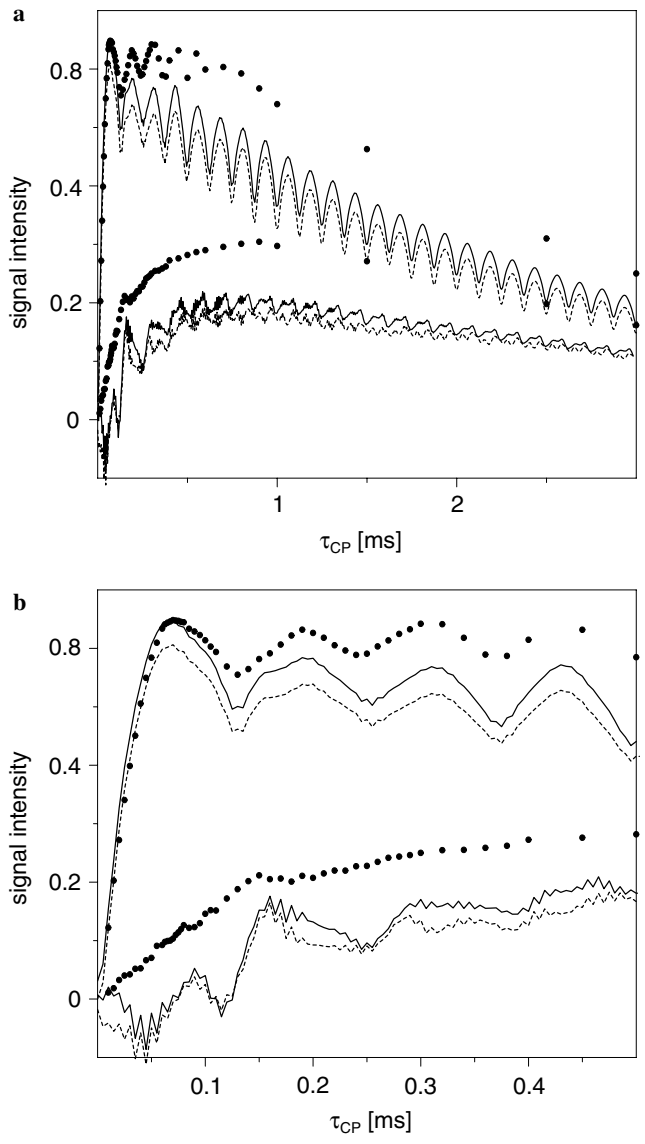

Fig. 5. The same as in Fig. 4, except that both, CH_3 and NH_3 moieties are assumed in a fast rotational regime.

deviations still exist even in the former case. A possible cause is represented by the limited size of the simulated system. However, this assumption seems rather implausible as it appears from comparing the seven and nine ^1H spins simulations (the dashed and continuous lines in the illustrated dependencies). Indeed, the additional two protons are seen to mostly affect the magnitude of the transferred polarization, while the overall shape of the buildup curve is kept almost unchanged (at least up to 0.5 ms—see Figs. 4b and Fig. 5b). Thus, the observed deviations are more likely indicative for NH_3 being in a slow rotational regime. Also, a small contribution coming from rf field inhomogeneity cannot be completely ruled out. Unfortunately, the employed simulation program is not yet adapted to incorporate slow molecular motion, so that the results illustrated in Fig. 4 set the accuracy level one can reach at the present stage. Finally, it is worth mentioning that the C-H9 simulations also provide a higher accuracy level in describing the polarization inversion process. Specifically, a better correspondence between the measured and computed ^{13}C polarization inversion time is obtained on the C-H9 system ($\tau_2 = 46$ μs), compared to C-H7 ($\tau_2 = 42$ μs).

The most important conclusion one can draw from the above analysis, is the increased sensitivity of remote protons CP/MAS to structural and dynamical details of distant protons. Indeed, very large deviations between simulated and measured remote protons polarization transfer curves have been obtained in this case under fast rotational assumption (Fig. 5) compared to a general good agreement that characterizes the rigid NH_3 approach (see Fig. 4). By contrast, the difference between the rigid-, and fast NH_3 rotation limit, is by far not so well pronounced in the case of conventional CP/MAS buildup curves. Nevertheless, the fact that conventional CP/MAS is less sensitive to details of the NH_3 molecular motion is not completely surprising, as these details can be easily obscured under the dominant effect of bonded proton. From practical perspective, the two polarization transfer schemes can be thus combined together to provide more structural and dynamical information than would result from using standard CP/MAS alone.

The derived results are important also from fundamental point of view. In particular, one has to remark the extended time-scale over which is valid the coherent description of cross-polarization dynamics within a relatively small spin cluster. This is already suggested by the good agreement between the simulated and measured conventional CP/MAS buildup curves up to 0.5 ms (Fig. 4b). However, the strongest arguments arise again from the analysis of remote protons CP/MAS, especially if one takes into account that a relatively long period (≈170 μs) of coherent manipulation of the ^1H spins has been applied prior to acquiring the corresponding buildup curve: yet, the agreement between the theoretical and experimental results is remarkably good in this case as well. This is, to some extent, in contrast to many theoretical descriptions of CP/MAS, where the surrounding protons are considered to form a strongly coupled spin reservoir that reaches rapid thermodynamic equilibrium after polarization transfer to the central ^{13}C has been accomplished.

Overall, one can conclude that the proposed scheme for polarization transfer from remote protons under CP/MAS is fully confirmed by the results obtained on L-alanine. A similar analysis has been performed for the CH_3 resonance, but the results will no longer be presented here from the following reasons: (i) as shown previously, the CPPI sequence cannot generate in this case an initial state suitable for pure remote protons CP/MAS (the corresponding curve will contain also a small contribution from directly bonded protons), and (ii) the measured (and simulated) CH_3 buildup curves do not provide essentially new insights into polarization transfer process compared to those already discussed on the example of CH group.

5. Conclusions

In the present work it was shown that polarization transfer from remote protons is possible if a suitable initial state of non-uniform polarization is prepared prior to record the CP/MAS buildup curve. By this procedure it was demonstrated that the coherent control of the spin system evolution can be extended over time scales longer than commonly considered in many theoretical treatments of CP/MAS. For instance, the present results are inconsistent with the assumption of a rapid thermal equilibrium reached within the abundant ^{1}H spins reservoir after the polarization has been transferred to the central carbon. With respect to possible practical applications of the proposed remote protons CP/MAS scheme, here, we refrained from getting into a very detailed investigation. Nevertheless, the findings of the present analysis are encouraging. In particular, this procedure was shown to: (i) represent a quick and convenient alternative for separating different contributions to the total transferred polarization, which is applicable when poor ^{1}H resolution prevents us from employing more sophisticated techniques, like 3D LG-CP HETCOR, (ii) show increased sensitivity to structural and dynamical details of distant protons, and (iii) provide information that, in combination with the results of standard CP/MAS, can lead to a better structural and dynamical characterization of organic solids. The present practical implementation of the proposed scheme, where the required initial state is prepared by means of the CPPI sequence, enables one to approach an ideal remote protons polarization transfer for CH group only. However, further improvements, either to its preparation part, or during the CP/MAS buildup curve acquisition (as suggested in Section 2), could in principle extend the practical applicability of this scheme.

Acknowledgment

Financial support from the Romanian Ministry of Education and Research (project CEEX05-D11-31) is gratefully acknowledged.

References

[1] S.R. Hartmann, E. Hahn, Nuclear double resonance in the rotating frame, Phys. Rev. 128 (1962) 2042–2053.
[2] J. Schaefer, E.O. Stejskal, R.A. McKay, High-resolution slow-spinning magic-angle carbon-13 NMR, J. Magn. Reson. 25 (1977) 569–573.
[3] M. Mehring, Principles of High Resolution NMR in Solids, Springer-Verlag, Berlin, 1983.
[4] A. Pines, M.G. Gigbby, J.S. Waugh, Proton-enhanced NMR of dilute spins in solids, J. Chem. Phys. 59 (1973) 569–590.
[5] M.H. Levitt, D. Suter, R.R. Ernst, Spin dynamics and thermodynamics in solid-state NMR cross-polarization, J. Chem. Phys. 84 (1986) 4243–4255.
[6] D.E. Demco, J. Tegenfeldt, J.S. Waugh, Dynamics of cross relaxation in nuclear magnetic double resonance, Phys. Rev. B 11 (1975) 4133–4151.
[7] E.O. Stejskal, J. Schaefer, J.W. Waugh, Magic-angle spinning and polarization transfer in proton enhanced NMR, J. Magn. Reson. 28 (1977) 105–112.
[8] D. Marks, S. Vega, A theory for cross-polarization NMR of nonspinning and spinning samples, J. Magn. Reson. A 118 (1996) 157–172.
[9] S.C. Shekar, A. Ramamoorthy, The unitary evolution operator for cross-polarization schemes in NMR, Chem. Phys. Lett. 342 (2001) 127–134.
[10] S.C. Shekar, A. Ramamoorthy, R.J. Wittebort, Determination of the chemical shielding tensor orientation from two or one of the three conventional rotations of a single crystal, J. Magn. Reson. 155 (2002) 257–262.
[11] M. Eden, B.H. Meier, Time-reversal of cross-polarization in nuclear magnetic resonance, J. Chem. Phys. 108 (1998) 9611–9613.
[12] L. Müller, A. Kumar, T. Baumann, R.R. Ernst, Transient oscillations in NMR cross-polarization experiments in solids, Phys. Rev. Lett. 32 (1974) 1402–1406.
[13] C.H. Wu, A. Ramamoorthy, S.J. Opella, High-resolution heteronuclear dipolar solid-state NMR spectroscopy, J. Magn. Reson. A 109 (1994) 270–272.
[14] A. Ramamoorthy, Y. Wei, D.K. Lee, PISEMA solid-state NMR spectroscopy, Annu. Rep. NMR Spectrosc. 52 (2004) 1–52.
[15] K. Hester, J.L. Ackerman, B.L. Neff, J.S. Waugh, Separated local field spectra in NMR: determination of structure of solids, Phys. Rev. Lett. 36 (1976) 1081–1083.
[16] P. Palmas, P. Tekely, D. Canet, Local-field measurements on powder samples from polarization inversion of the rare-spin magnetization, J. Magn. Reson. A 104 (1993) 26–36.
[17] A. Ramamoorthy, S.J. Opella, Two-dimensional chemical shift/heteronuclear dipolar coupling spectra obtained with polarization inversion spin exchange at the magic angle and magic-angle sample spinning (PISEMAMAS), Solid-State NMR 4 (1995) 387–392.
[18] K. Yamamoto, D.K. Lee, A. Ramamoorthy, Broadband-PISEMA solid-state NMR spectroscopy, Chem. Phys. Lett. 407 (2005) 289–293.
[19] V. Ladizhansky, S. Vega, Polarization transfer dynamics in Lee–Goldburg cross polarization nuclear magnetic resonance experiments on rotating solids, J. Chem. Phys. 112 (2000) 7158–7168.
[20] J. Brus, J. Jakes, Geometry of multiple-spin systems as reflected in ^{13}C–{^{1}H} dipolar spectra measured at Lee-Goldburg cross-polarization, Solid-State NMR 27 (2005) 180–191.
[21] S.V. Dvinskikh, H. Zimmermann, A. Maliniak, D. Sandström, Heteronuclear dipolar recoupling in solid-state nuclear magnetic resonance by amplitude-, phase-, and frequency-modulated Lee-Goldburg cross-polarization, J. Chem. Phys. 122 (2005), 044512:1–12.
[22] M. Hong, X. Yao, K. Jakes, D. Huster, Investigation of molecular motions by Lee-Goldburg cross-polarization NMR spectroscopy, J. Phys. Chem. B 106 (2002) 7355–7364.
[23] D.K. Lee, T. Narasimhaswamy, A. Ramamoorthy, PITANSEMA, a low-power PISEMA solid-state NMR experiment, Chem. Phys. Lett. 399 (2004) 359–362.
[24] K. Yamamoto, V.L. Ermakov, D.K. Lee, A. Ramamoorthy, PITANSEMA-MAS, a solid-state NMR method to measure heteronuclear dipolar couplings under MAS, Chem. Phys. Lett. 408 (2005) 118–122.
[25] S.V. Dvinskikh, K. Yamamoto, A. Ramamoorthy, Separated local field NMR spectroscopy by windowless isotropic mixing, Chem. Phys. Lett. 419 (2006) 168–173.
[26] K. Yamamoto, S.V. Dvinskikh, A. Ramamoorthy, Measurement of heteronuclear dipolar couplings using a rotating frame solid-state NMR experiment, Chem. Phys. Lett. 419 (2006) 533–536.
[27] C.H. Wu, A. Ramamoorthy, L.M. Gierasch, S.J. Opella, Simultaneous characterization of the amide ^{1}H chemical shift, ^{1}H–^{15}N dipolar, and ^{15}N chemical shift interaction tensors in a peptide bond by three-dimensional solid-state NMR spectroscopy, J. Am. Chem. Soc. 117 (1995) 6148–6149.

[28] R. Jelinek, A. Ramamoorthy, S.J. Opella, High-resolution three-dimensional solid-state NMR spectroscopy of a uniformly 15N-labeled protein, J. Am. Chem. Soc. 117 (1995) 12348–12349.
[29] A. Ramamoorthy, C.H. Wu, S.J. Opella, Three-dimensional solid-state NMR experiment that correlates the chemical shift and dipolar coupling frequencies of two heteronuclei, J. Magn. Reson. B 107 (1995) 88–90.
[30] B.J. van Rossum, C.P. de Groot, V. Ladizhansky, S. Vega, J.M. de Groot, A method for measuring heteronuclear (^{1}H–^{13}C) distances in high speed MAS NMR, J. Am. Chem. Soc. 122 (2000) 3465–3472.
[31] X. Wu, S.T. Burns, K. Zilm, Spectral editing in CPMAS NMR. Generating subspectra based on proton multiplicities, J. Magn. Reson. A 111 (1994) 29–36.
[32] M. Veshtort, R.G. Griffin, Spinevolution: A powerful tool for the simulation of solid and liquid state NMR experiments, J. Magn. Reson. 178 (2006) 248–282.
[33] M.S. Lehmann, T.F. Koetzle, W.C. Hamilton, Precision neutron diffraction structure determination of protein and nucleic acid components. I. Crystal and molecular structure of the amino acid L-alanine, J. Am. Chem. Soc. 94 (1972) 2657–2660.
[34] L.F. Power, K.E. Turner, F.H. Moore, The crystal and molecular structure of α-glycine by neutron diffraction—a comparison, Acta Cryst. B32 (1976) 11–16.
[35] Z. Gu, K. Ebisawa, A. McDermott, Hydrogen bonding effects on amine rotation rates in crystalline amino acids, Solid-State NMR 7 (1996) 161–172.